Topical Review

The micro-mechanics of single molecules studied with atomic force microscopy

Thomas E. Fisher, Piotr E. Marszalek, Andres F. Oberhauser, Mariano Carrion-Vazquez and Julio M. Fernandez

Department of Physiology and Biophysics, Mayo Foundation, 1-117 Medical Sciences Building, Rochester, MN 55905, USA

(Received 29 April 1999; accepted after revision 14 June 1999)

The atomic force microscope (AFM) in its force-measuring mode is capable of effecting displacements on an angstrom scale (10 Å = 1 nm) and measuring forces of a few piconewtons. Recent experiments have applied AFM techniques to study the mechanical properties of single biological polymers. These properties contribute to the function of many proteins exposed to mechanical strain, including components of the extracellular matrix (ECM). The force-bearing proteins of the ECM typically contain multiple tandem repeats of independently folded domains, a common feature of proteins with structural and mechanical roles. Polysaccharide moieties of adhesion glycoproteins such as the selectins are also subject to strain. Force-induced extension of both types of molecules with the AFM results in conformational changes that could contribute to their mechanical function. The force–extension curve for amylose exhibits a transition in elasticity caused by the conversion of its glucopyranose rings from the chair to the boat conformation. Extension of multi-domain proteins causes sequential unraveling of domains, resulting in a force–extension curve displaying a saw tooth pattern of peaks. The engineering of multimeric proteins consisting of repeats of identical domains has allowed detailed analysis of the mechanical properties of single protein domains. Repetitive extension and relaxation has enabled direct measurement of rates of domain unfolding and refolding. The combination of site-directed mutagenesis with AFM can be used to elucidate the amino acid sequences that determine mechanical stability. The AFM thus offers a novel way to explore the mechanical functions of proteins and will be a useful tool for studying the micro-mechanics of exocytosis.

Exocytotic fusion is, in essence, a mechanical event. Each of the major steps in secretion (transport of vesicles, docking with the exocytotic machinery, apposition with the plasma membrane and fusion) entails physical movement and the generation of force. The ability to measure directly the micro-mechanics of exocytosis would provide a new way to study the functions of, and relationships between, the proteins involved. With the development of the force-measuring mode of the atomic force microscope (AFM), it is now possible to conceive of such experiments. Does an interaction between vesicular and plasmalemmal proteins generate a force that serves to bring the two membranes together? Could this interaction be activated or regulated by Ca^{2+}? Could a third protein inhibit the interaction in a Ca^{2+}-dependent fashion? Although experiments on exocytotic proteins have not yet been attempted, the AFM has been used to study the elastic properties of proteins with mechanical functions. These include the muscle protein titin (Rief *et al.* 1997*a*, 1998) and the extracellular matrix (ECM) protein tenascin (Oberhauser *et al.* 1998). The ECM in particular provides an excellent framework in which to study the mechanical properties of polymers since so much is known about the proteins involved and their specific functions (e.g. Alon *et al.* 1995; Palecek *et al.* 1997). This review will discuss a recent series of experiments in which the AFM was used to probe the elasticity of single biological polymers to better understand the function of the ECM. These experiments provide a road map for the study of the mechanical properties of single biological polymers, as well as the generation of force by the interaction between protein molecules. They may therefore illuminate ways in which the AFM may be applicable to the study of exocytosis.

Presented at The Journal of Physiology Symposium on Secretion: Mechanisms and Regulation of Exocytosis, Washington DC, 17 April 1999.

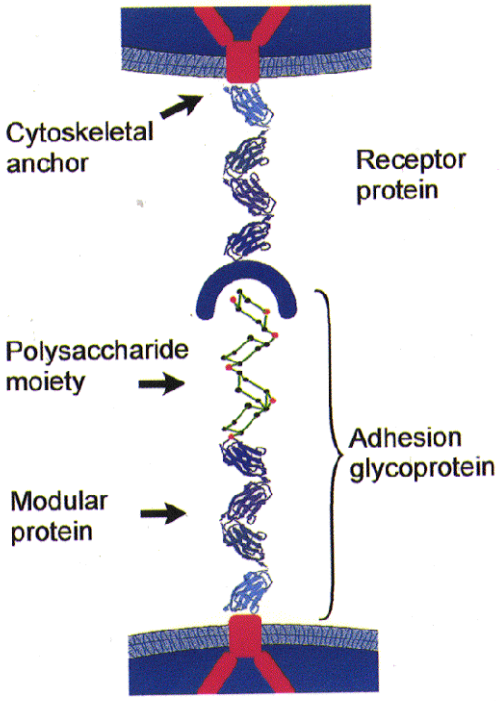

Figure 1. The elastic components of cell adhesion interactions
An idealized representation of the components in a cell–cell interaction. A glycoprotein consisting of multiple extensible domains and a polysaccharide moiety interacts with a receptor protein on a neighbouring cell that also contains multiple extensible domains.

The ECM forms the mechanical attachment between cells. Connections are formed by the interaction of proteins on adjacent cells or, as in the case of the selectins, by the interaction of the polysaccharide moiety of a glycoprotein with a receptor protein on a neighbouring cell (Chothia & Jones, 1997; see Fig. 1). ECM proteins are firmly anchored to the cytoskeleton and form an integrated network that is under constant, and constantly changing, tension (Chicurel *et al.* 1998). The ECM is a dynamic scaffold that transduces mechanical signals to regulate processes such as growth, differentiation and synaptic plasticity. One of the most prominent features of ECM proteins is that they are composed of multiple copies of individually folded domains (Hynes, 1999), which appears to be a common feature of proteins involved in mechanical function. Fibronectin contains three types of repeating domains, known as fibro-

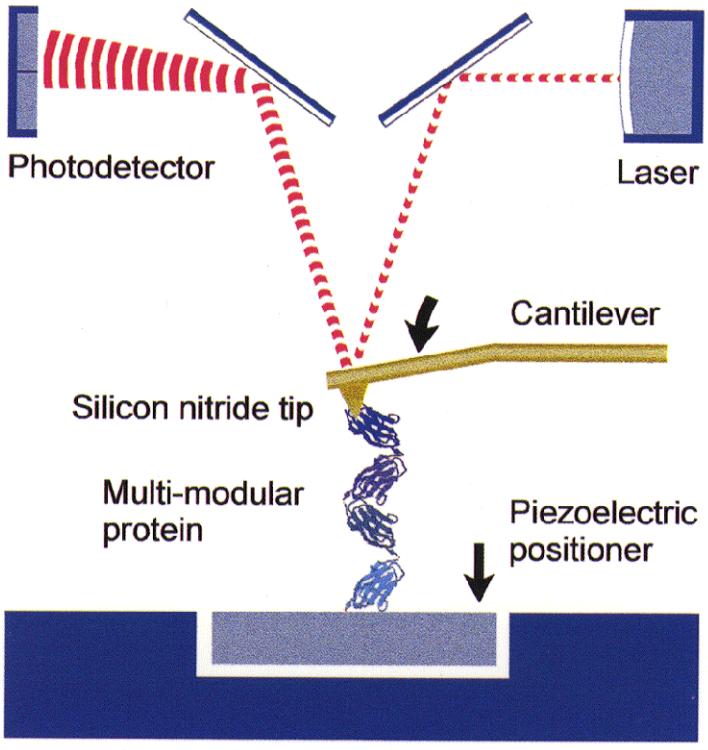

Figure 2. The AFM in its force–extension mode
Extension of a single molecule caused by retraction of the piezoelectric positioner results in deflection of the cantilever. This deflection changes the angle of reflection of a laser beam striking the cantilever, which is measured as the change in output from a photodetector.

nectin domains I, II and III. The type III repeat (FN-III) is the one of the most widespread peptide modules and is found in an estimated 2% of all animal proteins (Bork & Doolittle, 1992). Recent experiments with a fibronectin–green fluorescent protein chimera have demonstrated that fibronectin is highly elongated in the ECM and suggest that the tension in the ECM may result in the force-induced unfolding of individual fibronectin domains (Ohashi *et al.* 1999). Mechanically induced conformational changes, in both proteins and polysaccharide molecules, may thus be important in ECM function.

The first demonstration of the ability of the AFM to measure elasticity at a molecular level occurred in 1997, with the extension of single dextran molecules (Rief *et al.* 1997*b*). Since that time, the method has proved to be capable of stretching a variety of biological polymers, including polysaccharides (Rief *et al.* 1997*b*; Marszalek *et al.* 1998), proteins (Rief *et al.* 1997*a*, 1998; Oberhauser *et al.* 1998; Carrion-Vazquez *et al.* 1999) and DNA (Rief *et al.* 1999), with exquisite precision. This technique is now poised to open a new field of inquiry – single molecule force spectroscopy – that will enable an unprecedented view of the mechanical properties and functions of biological polymers.

The atomic force microscope

The original and more familiar use of the AFM is for the measurement of the surface contours of a microscopic sample (Binnig *et al.* 1986; Shao & Yang, 1995; Hansma & Pietrasanta, 1998). A microscopic silicon nitride tip mounted on a cantilever is skimmed over the surface in a raster pattern. The tip rises and falls depending on the contour of the sample, much like the stylus on a record player. By bouncing a laser beam off the top of the cantilever onto a

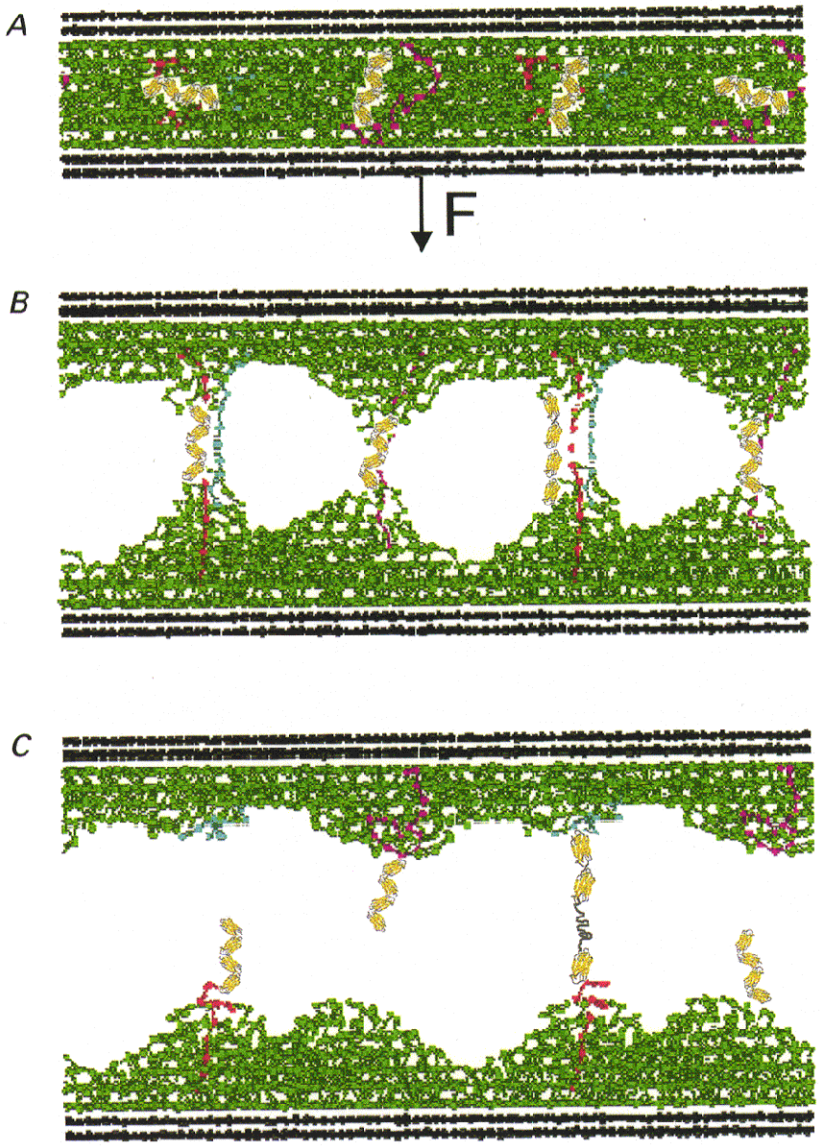

Figure 3. Inter-molecular interactions at the AFM cantilever tip

A hypothetical series of events as an AFM tip is pressed against a layer of polymers and then withdrawn. Modified from Baljon & Robbins, 1996. F, force.

photodetector, the angle of the cantilever, and thus the height of the surface that it is contacting, can be measured. By collating the information from the entire surface, the contour of the sample can be reconstructed. In the force-measuring mode of the AFM (Czajkowsky & Shao, 1998), deflections result from the forced extension of a sample attached to the cantilever tip. In this configuration, the cantilever is mounted above an absorptive substrate whose height is controlled by a single axis piezoelectric positioner with angstrom resolution. When the ends of a single polymer are adsorbed between the cantilever and a substrate, recession of the substrate causes elongation of the polymer, resulting in a force that causes deflection of the cantilever (see Fig. 2). As with conventional AFM, the deflection is measured by bouncing a laser beam off the cantilever onto a photodetector. By calibrating the spring constant of the cantilever, the deflection can be used to measure the relationship between extension and force for a single polymer molecule. Formation of such an arrangement is accomplished by pressing the cantilever tip against a layer of the polymer adsorbed to the substrate. The probable steps in the capture of a single multi-domain protein are illustrated in Fig. 3. Panel *A* shows the compression of the protein layer as the tip is pressed against it. As the substrate is withdrawn (panel *B*) some of the molecules are adsorbed to the tip. The bonds between the two layers are gradually broken until a single protein forms the only connection between the two surfaces. On further extension, the independent domains of the protein begin to unfold (panel *C*).

Analysis of polymer elasticity

When a biological polymer is elongated using mechanical force, the results may be plotted as a force–extension curve. At zero force, polymer chains exist in a coiled state, as this maximizes their conformational freedom (entropy). Extending a relaxed chain generates an opposing force that is predicted from the reduction in entropy. This effect is known as entropic elasticity and may be interpreted using a model of polymer elasticity called the freely jointed chain (FJC) model. In its simplest case, a polymer is modelled as a chain of equal, independent and freely rotating segments. A parameter for elasticity of the segments may also be incorporated, and this equation is shown in Fig. 4. The model therefore describes the elastic behaviour of polymers based on three adjustable parameters: the contour length of the molecule (L_c), the Kuhn length (l_K), and the elasticity of the segments (K_s). The contour length refers to the full, but not elongated, length of the polymer, the Kuhn length to the size of the independent segments, and the segment elasticity to the resistance to extension. The force–extension relationship for a hypothetical polymer with a contour length of 100 nm, a Kuhn length of 1 nm, and a very low extensibility ($K_s = 10^9$ pN nm^{-1}), is shown by the black line in Fig. 4. This molecule has a low resistance to extension until the polymer is near its contour length, at which point the force necessary to extend further rises rapidly. Each of the coloured lines shows the relationship when one of the three parameters is altered. An increase in contour length causes a parallel shift in the curve to the right (red line). Making the polymer more elastic by reducing the K_s results in a molecule that will extend beyond its contour length when exposed to high force (blue line). Finally, decreasing the Kuhn length, which increases the number of segments and therefore the entropy of the polymer, results in a greater resistance to extension at low forces.

Stretching polysaccharides

The force-measuring mode of the AFM was first used to measure the bond forces between avidin and biotin (Florin *et al.* 1994; Moy *et al.* 1994), an antigen and an antibody

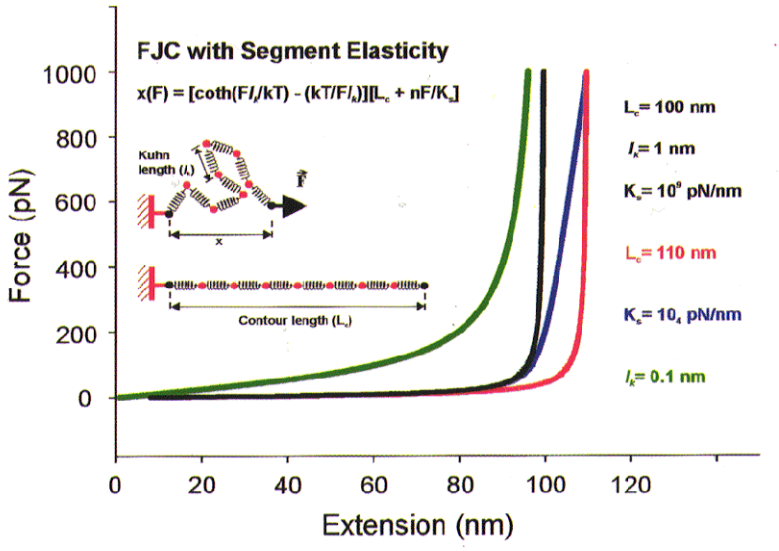

Figure 4. The freely jointed chain model of polymer elasticity

The force–extension relationships for a series of hypothetical polymers constructed using the FJC equation (see inset for equation and illustration of parameters). The relationship for a set of given values (plot and parameters shown in black) are changed by a single parameter for each of the other three plots (colours).

(Dammer *et al.* 1996; Hinterdorfer *et al.* 1996), and between two complementary strands of DNA (Lee *et al.* 1994). The applicability of this method to the extension of single molecules was first demonstrated using polysaccharides (Rief *et al.* 1997*b*). Single molecules of carboxymethylated dextran with lengths from 50 nm to 2 μm were elongated by the AFM and were found to undergo a marked transition in elasticity at forces above 250 pN. The molecular events underlying this transition were recently identified by Marszalek *et al.* (1998). It was observed that a variety of polysaccharides derived from glucopyranose (including amylose, see Fig. 5*A*) undergo a similar transition, although at different forces. The force–extension curve for amylose, shown in Fig. 5*B* (dark line), clearly shows an abrupt alteration when about 300 pN of force is applied. The thin traces in Fig. 5*B* show fits of the FJC model to the low force ($I_{\min}$) and high force ($I_{\max}$) portions of the curve. The transition represents a molecular rearrangement (a change in enthalpy) resulting in a change in the elastic properties of the polysaccharide. Before the transition, the optimal Kuhn length to fit the data is close to the length of a single glucopyranose ring. Following the transition, the Kuhn length is longer, and the extensibility is decreased. The change in molecular conformation that underlies this transition was revealed by a mild oxidation with periodate. Periodate treatment breaks bonds between two hydroxylated carbons, and therefore cleaves the glucopyranose ring in amylose and similar polysaccharides. The result of this treatment on the force–extension curve is a gradual disappearance of the enthalpic component. This strongly suggests that the transition in amylose elasticity is caused by a change in conformation of the polysaccharide ring. Molecular modelling suggests that this result may be explained by conversion of the glucopyranose ring from the favoured chair conformation to the longer boat conformation (see inset to 5*B*). Monte Carlo simulations of force-induced unfolding of amylose yields a similar force–extension curve (Fig. 5*C*). In polysaccharides with glycosidic linkages similar to that of amylose, this conformation change causes an increase in the distance between the consecutive glycosidic oxygen molecules (see inset to Fig. 5*B*). Polysaccharides in which conversion from the chair to the boat conformation does not lengthen the molecule, do not show a measurable enthalpic component in their force–extension curves (Marszalek *et al.* 1998; Li *et al.* 1998). This supports the interpretation that the transition in amylose elasticity is caused by a conformational change in the glucopyranose ring. If similar polysaccharide linkages exist in glycoproteins involved in cell–cell adhesion, this change might contribute to the elastic properties of the interaction. Furthermore, a conformational change could alter the binding of a polysaccharide moiety to a receptor molecule, and thereby act as a signalling mechanism activated by mechanical stress.

Unfolding protein domains

Unfolding of protein domains with the AFM was first demonstrated using the giant muscle protein titin (Rief *et al.* 1997*a*). Titin is an extensible protein that is responsible for the passive elasticity of muscle. It has a molecular mass of greater than 1000 kDa and is composed mostly of individually folded domains of the immunoglobulin (Ig) and FN-III type. Although these modules differ greatly in amino acid sequence, they share a seven-stranded β-barrel structure. It has been proposed that unfolding and refolding of these domains explains the elasticity of the molecule (Erickson, 1994). Titin thus provides an ideal subject with which to study mechanically induced unfolding.

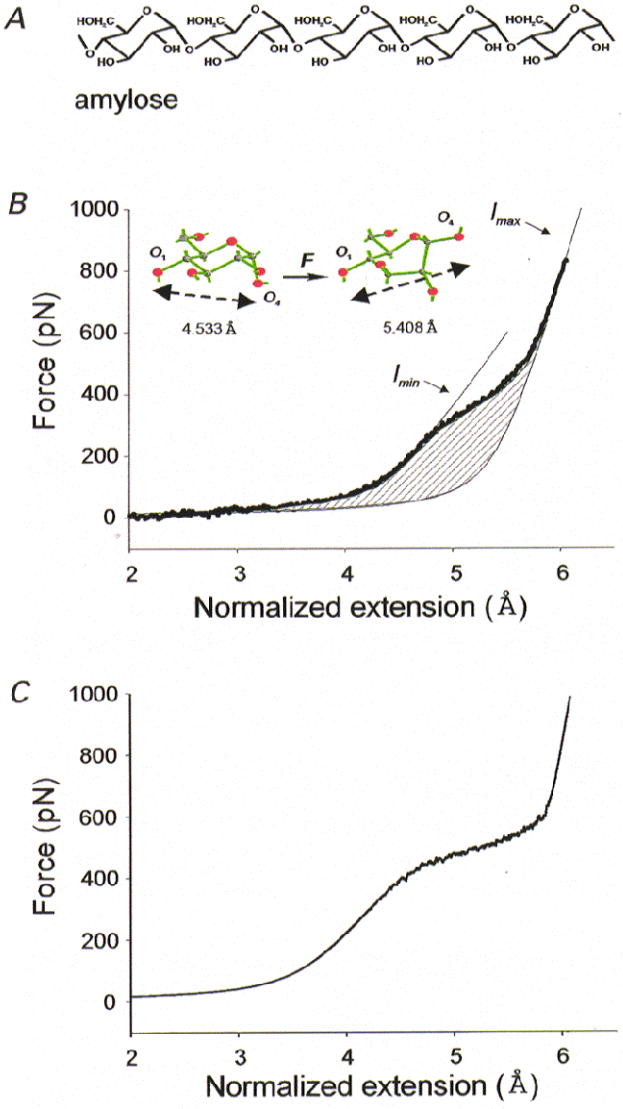

Figure 5. Force-induced conformational changes in amylose

A, diagram of the structure of amylose. *B*, force–extension curve for amylose (dark line). The thin lines show fits of the low force portion ($I_{\min}$) and the high force portion ($I_{\max}$) to the FJC model. Inset shows the conversion of the glucopyranose ring from the chair to the boat conformation with its attendant increase in length. *C*, a Monte Carlo simulation of the force-induced conformational change in amylose reproduces the main features of the experimental data. Adapted from Marszalek *et al.* 1998. 10 Å = 1 nm.

The first direct observations of domain unfolding were made using a recombinant protein that consisted of eight tandem Ig domains from human cardiac muscle titin (Rief *et al.* 1997*a*). This protein was constructed by PCR amplification of a portion of human cardiac titin encompassing the eight Ig modules I27–I34. AFM measurements of the elasticity of this protein showed force–extension curves with a saw tooth pattern of up to eight peaks with a periodicity between 25 and 28 nm (similar to the results illustrated in Fig. 6*A* and *B*). As the protein begins to be stretched, the resisting force is that required to decrease the entropy of the protein. At greater extensions, the probability for the unfolding of individual domains becomes very high. When a domain unfolds, the AFM tip relaxes back toward its resting position and the force decreases to near zero. The saw tooth pattern thus reflects the sequential unfolding of individual Ig domains.

The elasticity of a polypeptide chain may be described by the worm-like chain (WLC) model of polymer elasticity, which is similar to the FJC model but does not assume that the segments are fully independent. The adjustable parameters are the persistence length (which defines the flexibility of the peptide) and the contour length. Module unfolding has a dramatic effect on both parameters. The resultant change in contour length can be used to calculate the size of the folded domain. While the persistence length in the folded state is influenced by the size of the domains (which for titin are about 4 nm), that following unfolding reflects the size of the constituent amino acids (about

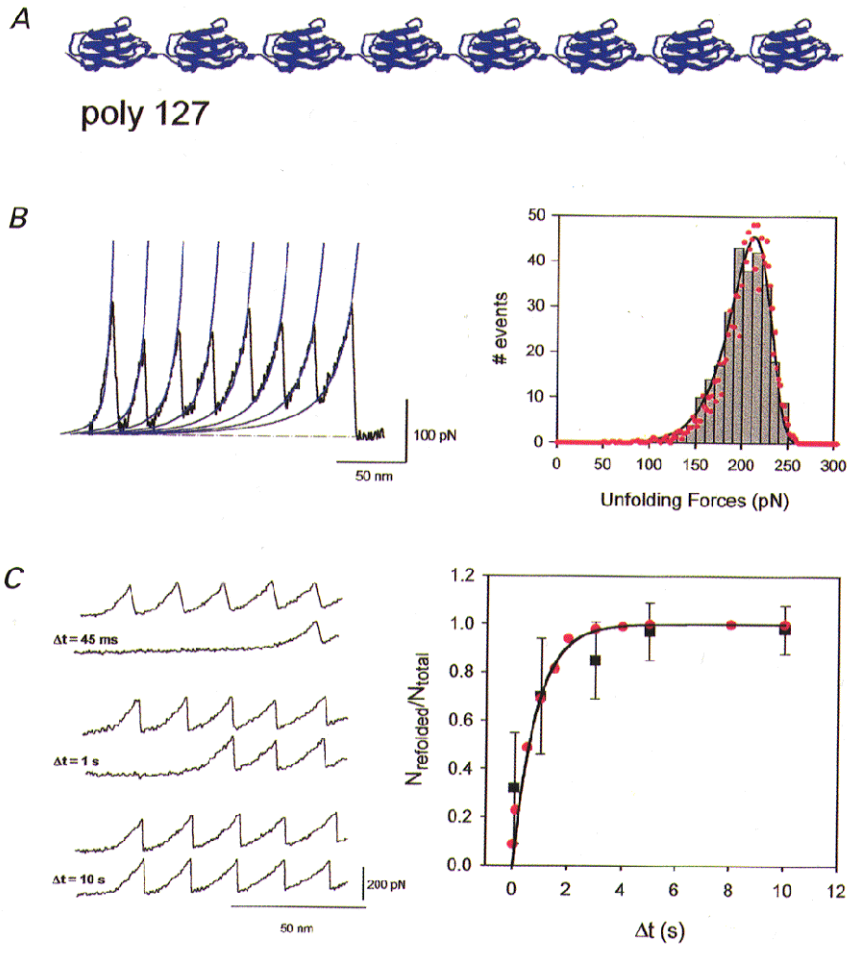

Figure 6. Force-induced unfolding of recombinant poly I27

A, schematic diagram of the repeating, independently folded domains of poly I27. *B*, force–extension curve for poly I27 unfolding with fits to the WLC model for each of the peaks. On the right is a frequency histogram for the unfolding of I27. The red circles are the results of a Monte Carlo simulation (see text for values). *C*, unfolding and refolding kinetics of $I27^{RS}{}_{8}$ probed with a double-pulse protocol. The three pairs of traces are from a single molecule in which five domains are stretched between tip and substrate. When the molecule is stretched twice in succession with a variable delay, there is a variable number of peaks in the second extension (bottom traces of each pair). This corresponds to the time dependence of refolding (see text). On the right is a plot of the proportion refolded ($N_{refolded}/N_{total}$) *versus* time interval (Δt). The black line is a fit of the data and the red circles are from a Monte Carlo simulation of a two state folding/unfolding kinetic model (see text for further details). Panel *B* is taken from Carrion-Vazquez *et al.* 1999.

0·38 nm). Titin domains unfold in a hierarchical sequence, with a larger force required for each consecutive unfolding event (Rief *et al.* 1997*a*). This suggests that the domains of titin are structured to unfold in a specific order. These experiments also showed that unfolding occurs as a probabilistic event. This means that unfolding does not occur after a 'threshold force', but rather that the probability of unfolding increases with applied force.

These properties are not limited to titin. Many of the same phenomena were observed with the mechanically induced unfolding of the ECM protein tenascin (Oberhauser *et al.* 1998). This demonstrates that the unfolding properties observed for the Ig modules of titin are similar to those observed for the FN-III domains of tenascin. This is particularly interesting since the FN-III domain is such a common structural motif in modular proteins (Bork & Doolittle, 1992). Furthermore, these data suggest that domain unfolding could be an important determinant of elasticity in ECM proteins and that the elastic properties of proteins could play a role in cell–cell interactions.

The unfolding of multiple protein domains may also contribute to mechanisms of biological adhesion (Smith *et al.* 1999). The remarkable fracture resistance of the abalone shell is formed by alternating microscopic layers of crystalline calcium carbonate with protein-containing organic material. When a shell is cleaved to expose an organic layer and fastened to the base of an AFM, the cantilever tip can adsorb proteins that display a saw tooth pattern on their force–extension curves. This observation may represent an adaptation for proteins involved in adhesion. Formation of a connection using a multi-domain protein increases both the degree of extension over which the bond is maintained and the work that is required to break the bond (Oberhauser *et al.* 1998; Evans & Ritchie, 1999; Smith *et al.* 1999). The energy required for bond rupture is given by the area under the force–extension curve. For a bond formed by an inextensible molecule, the force curve will show a single sharp peak. The addition of multiple unfolding domains therefore increases the amount of work needed to break the bond. This may be a common mechanism by which natural adhesives and fibres resist breakage (Smith *et al.* 1999).

Polyproteins

The presence of multiple domains in a protein is a highly useful feature for the purpose of AFM studies. It is difficult to work with short proteins because the non-specific interactions between the cantilever tip and the polymer layer obscure the forces of interest at short extensions (see Fig. 3). Also, when a single unfolding event does occur it may be difficult to distinguish from non-specific interactions. A saw tooth pattern is a clear signal that the measured force–extension curve is derived from the modular protein of interest. The common features of the unfolding pathway are also amplified, allowing for identification and measurement of small conformational changes. With a native protein or protein fragment, however, there are usually no means to identify which peaks correspond to which protein domains. It is therefore impossible to define the characteristics of a specific domain. Subtle differences between the domains may also be difficult to detect, particularly if only one or two of the peaks display a unique feature. These problems have been addressed by the construction of modular polyproteins with identical repeating domains using molecular biological techniques. This has enabled direct measurement of the unfolding–refolding properties of a single protein domain. The summation of events that occur prior to unfolding, as well as the repetition of the unfolding events themselves, make polyprotein construction a powerful tool for the identification of the processes underlying mechanical unfolding. The production of homomeric polyproteins has also allowed a direct comparison between unfolding events induced by chemical denaturation and those induced mechanically (see below). Site-directed mutagenesis of constructed polyproteins will help to identify the specific amino acid sequences involved in mechanical stability. This strategy will exploit structural information on the domains derived from other sources, such as NMR, as well as from molecular dynamics simulations.

The first polyprotein was constructed from I27, an 89 amino acid Ig domain that was part of the titin fragment used in the original AFM experiments on titin (Rief *et al.* 1997*a*). It was chosen in part because its structure has been described using NMR (Improta *et al.* 1996), it has a known thermodynamic stability (Politou *et al.* 1995), and its conformational changes in response to an applied force has been modelled using a steered molecular dynamics simulation (Lu *et al.* 1998). Two methods were used to synthesize and express recombinant multimers of I27, with similar results. Both methods resulted in a sequence of eight I27 domains each linked by two amino acids (Carrion-Vazquez *et al.* 1999; Fig. 6*A*). The results of stretching one of the constructs, which has arginine–serine as a linker and is therefore called $I27^{RS}{}_8$, is illustrated in Fig. 6*B*. The force–extension curves of $I27^{RS}{}_8$ are well described by the WLC model (blue lines). Fits of the WLC to the force–extension curves of $I27^{RS}{}_8$ gave a persistence length (p) of $0{\cdot}39 \pm 0{\cdot}07$ nm ($n = 10$), which is close to the size of a single amino acid (0·38 nm). Consecutive peaks were fitted by the WLC with the same persistence length and a contour length increment of $\Delta L_c = 28{\cdot}4 \pm 0{\cdot}3$ nm ($n = 16$). This value is approximately equal to the expected length of 89 fully extended amino acids minus the folded length of the module. Since the length of a single amino acid is about 0·38 nm, and the size of a folded I27 domain is 4·4 nm (Improta *et al.* 1998), the difference between folded and unfolded length should be $(89 \times 0{\cdot}38\ \text{nm}) - 4{\cdot}4\ \text{nm} = 29{\cdot}4$ nm. In contrast to the hierarchical pattern of unfolding seen with native protein fragments, a histogram of force peaks measured from 266 unfolding events reveals an asymmetrical distribution of events with a maximum at ~200 pN (Fig. 6*B*, right). The variations in the force required to unfold are stochastic, consistent with the idea that during stretching, the I27 modules unfold independently.

Remarkably, the AFM technique is also able to demonstrate the time dependence of domain refolding (Fig. 6*C*). This was accomplished using a double pulse experiment. The first extension of the polyprotein showed the number of available folded domains, which depends on the position of the attachments of the protein with the cantilever tip and the substrate. After reaching the extended state, the protein was relaxed to its initial length. After a variable interval the protein was stretched again and the number of force peaks was observed. The number of peaks in the second extension was found to depend exponentially on the amount of time that the protein remains relaxed (Fig. 6*C*, right). These results indicate the time dependence of the refolding reaction during relaxation. These data are well described as a simple first order folding reaction where the folding probability is given by $P_f(t) = 1 - e^{-t k_{f=0}}$, and the refolding rate at zero force, $k_{f=0}$, is equal to $1{\cdot}2\ s^{-1}$.

A Monte Carlo technique was used to simulate a chain of modules placed under force, and the forces required to unfold domains during the simulated extensions were compiled. The force applied to the modules was calculated from the WLC model of elasticity and varied depending on the contour length and the total extension of the protein (Rief *et al.* 1997*a*; Oberhauser *et al.* 1998). The unfolding and refolding of the modules was assumed to be a simple two-state reaction with rate constants that depend exponentially on the applied force (Rief *et al.* 1997*a*, 1998; Oberhauser *et al.* 1998). The distribution of unfolding forces measured from the I27 polyprotein were best fitted with an unfolding rate at zero force of $k_{u=0} = 3{\cdot}3 \times 10^{-4}\ s^{-1}$ and an unfolding distance $\Delta x_u = 0{\cdot}25$ nm. This suggests that the force required to unfold a domain is exerted over a very small distance, about the size of a water molecule. This is consistent with a steered molecular dynamics simulation suggesting that force-induced extension of I27 is resisted by a small number of hydrogen bonds and that breakage of these bonds causes a rapid unraveling of the entire domain (Lu *et al.* 1998).

The results of AFM denaturation may be compared with results obtained by standard chemical denaturation techniques. The stability of I27 was determined by equilibrium guanidinium chloride (GdmCl) denaturation (Carrion-Vazquez *et al.* 1999). Unfolding was monitored by observing the change in fluorescence at 320 nm (excitation at 280 nm). The fluorescence of the protein decreases significantly on unfolding. When the unfolding rate constant was extrapolated to 0 M denaturant, a value was obtained ($4{\cdot}9 \times 10^{-4}\ s^{-1}$) that is similar to that obtained from AFM experiments extrapolated to zero force ($3{\cdot}3 \times 10^{-4}\ s^{-1}$). Hence, the height of the unfolding energy barrier is similar in both cases (≈ 22 kcal mol^{-1}). These agreements are remarkable and suggest that the two methods are measuring a similar process. It remains to be seen whether this accordance will hold for a wide range of proteins or are specific for proteins that are designed to withstand axial

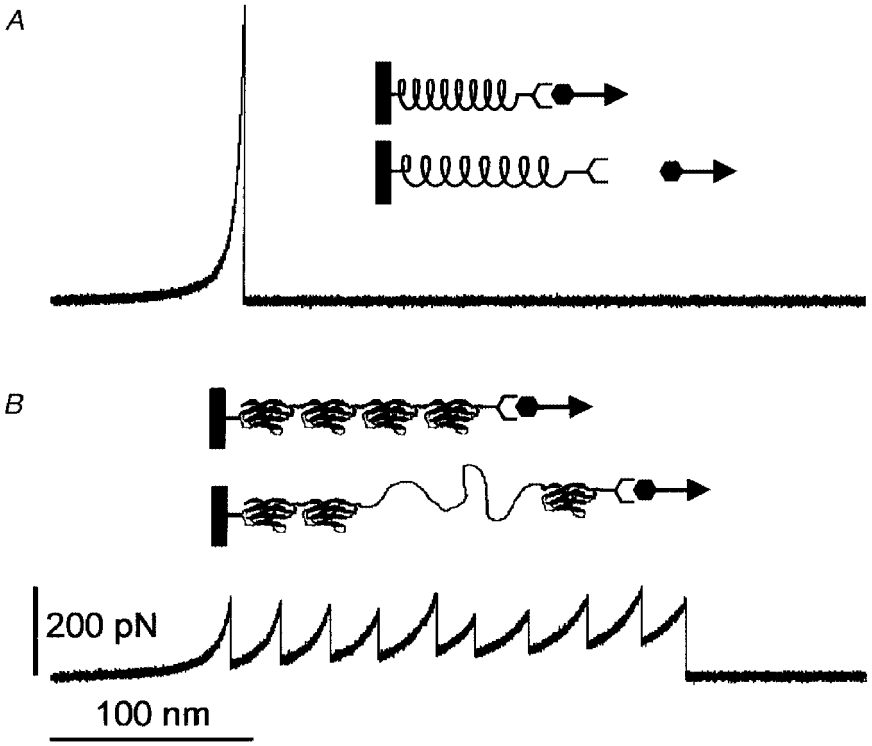

Figure 7. The influence of molecular elasticity on cell adhesion stability

A, simulation of a bound 100 nm long protein, without extensible modules, stretched at a speed of $0{\cdot}2$ nm ms^{-1}, predicts a force–extension curve where bond breakage occurs after a 90 nm extension at a force of 330 pN. *B*, at the same pulling speed, the simulated force–extension curve of a bound protein composed of 15 FN-III domains (inset; only 4 are shown) shows bond breakage after an extension of 268 nm at a force of 69 pN following unfolding of 9 of the domains. Adapted from Oberhauser *et al.* 1998.

stress. This agreement does not hold for the measured folding rates, which were smaller when measured by AFM than when estimated by extrapolating to 0 M denaturant (Carrion-Vazquez *et al.* 1999). This may be related to the decrease in degrees of rotational freedom of the domains in the AFM experiments caused by the tethering of the modules.

The utility of molecular biology in combination with AFM experiments has been demonstrated by the construction of polyproteins in which a number of glycines have been inserted at different points in the I27 sequence. These experiments demonstrate not only the precision of the AFM measurements but may also be used to probe the structure of the I27 fold (Carrion-Vazquez *et al.* 1999). The measured spaces between the peaks of unfolding a modular protein are thought to correspond to the increase in contour length of the protein caused by the unfolding of one of its modules (ΔL_c). In order to demonstrate the validity of this model and measure the sensitivity of the AFM, a cluster of five glycines was inserted into a loop within the folded structure of the module. As was predicted, unfolding of the I27–5Gly module revealed a ΔL_c that was larger by 1·9 nm (the length of 5 glycines; $\Delta\Delta L_c = 5 \times 0{\cdot}38$ nm $= 1{\cdot}9$ nm). In contrast, when glycines were inserted in a position that is between the proposed force-resisting hydrogen bonds of consecutive I27 folds, the interval between peaks was not affected. This is because the space between the folds is fully elongated before the domains begin to unfold. These results reveal the extraordinary capacity of the single molecule AFM technique to examine the mechanical properties of a protein module with amino acid resolution.

AFM experiments are also capable of illuminating rare folding events, not usually observed with other techniques. During repeated extension–relaxation cycles, the saw tooth pattern on the force–extension curves for $I27^{RS}{}_8$ sometimes showed missing force peaks (Oberhauser *et al.* 1999). This phenomenon differed from that seen in the time dependence of refolding experiments in that the missing peaks ('skips') were in the middle of the sequence of unfolding, between apparently normal examples of unfolding. This only occurred following induced unfolding; skips were never observed when a molecule was pulled for the first time. One possible interpretation is that skips represent folds in which two unfolded domains refold into a single larger fold with similar stability. This hypothesis was substantiated by the observation that the peak following the skip was offset by a distance that corresponded to one I27 domain plus the number of amino acids between the end of one I27 fold and the beginning of the next. Furthermore, the size of this offset could be altered by the insertion of glycines in the spacer even though, as described above, the interval between consecutive peaks was not normally altered by insertion of glycines within the spacer. The missing peaks therefore correspond to the unfolding of a structure formed by the interconnection of two I27 domains. Dimeric Ig folds have been described in an isolated Ig domain of the adhesion protein CD2 (Murray *et al.* 1998).

Conclusions

Measurement of force-induced elongation with the AFM can determine the mechanical properties of proteins and polysaccharides with exquisite sensitivity. Such studies will offer a new perspective in the identification and characterization of mechanical functions of proteins. A simple example of how molecular elasticity may influence protein interactions is illustrated in Fig. 7. If a receptor is attached to an elastic, multimodular protein, the interaction will be maintained over a much greater extension, and the rupture of the bond will occur at a lower force. These properties may prove to be vital for the function of extracellular matrix proteins in mediating cell–cell interactions. Furthermore, they may also be important in other types of attachment interactions such as the docking of vesicles to the exocytotic machinery.

The utility of the AFM in studying the processes of exocytosis is an exciting, but untested possibility. Using constructed polyproteins, it may be possible to test directly models describing the function of the exocytotic machinery, such as the recently proposed SNAREpin hypothesis (Weber *et al.* 1998). As the proteins involved in secretion become better understood, the AFM will provide a useful tool for elucidating their function.

Alon, R., Hammer, D. A. & Springer, T. A. (1995). Lifetime of the P-selectin-carbohydrate bond and its response to tensile force in hydrodynamic flow. *Nature* **374**, 539–542.

Baljon, A. R. C. & Robbins, M. O. (1996). Energy dissipation during rupture of adhesive bonds. *Science* **271**, 482–484.

Binnig, G., Quate, C. F. & Gerber, C. (1986). Atomic force microscope. *Physical Review Letters* **56**, 930–933.

Bork, P. & Doolittle, R. F. (1992). Proposed acquisition of an animal protein domain by bacteria. *Proceedings of the National Academy of Sciences of the USA* **89**, 8990–8994.

Carrion-Vazquez, M., Marszalek, P. E., Oberhauser, A. F. & Fernandez, J. M. (1999). AFM captures length phenotypes in single proteins. *Proceedings of the National Academy of Sciences of the USA* (in the Press).

Carrion-Vazquez, M., Oberhauser, A. F., Fowler, S. B., Marszalek, P. E., Broedel, S. E., Clarke, J. & Fernandez, J. M. (1999). Mechanical and chemical unfolding of a single protein: A comparison. *Proceedings of the National Academy of Sciences of the USA* **96**, 3694–3699.

Chicurel, M. E., Chen, C. S. & Ingber, D. E. (1998). Cellular control lies in the balance of forces. *Current Opinion in Cell Biology* **10**, 232–239.

Chothia, C. & Jones, E. Y. (1997). The molecular structure of cell adhesion molecules. *Annual Review of Biochemistry* **66**, 823–862.

Czajkowsky, D. M. & Shao, Z. (1998). Submolecular resolution of single macromolecules with atomic force microscopy. *FEBS Letters* **430**, 51–54.

Dammer, U., Hegner, M., Anselmetti, D., Wagner, P., Dreier, M., Huber, W. & Guntherodt, H. J. (1996). Specific antigen/antibody interactions measured by force microscopy. *Biophysical Journal* **70**, 2437–2441.

Erickson, H. P. (1994). Reversible unfolding of fibronectin type III and immunoglobulin domains provides the structural basis for stretch and elasticity of titin and fibronectin. *Proceedings of the National Academy of Sciences of the USA* **91**, 10114–10118.

Evans, E. & Ritchie, K. (1999). Strength of a weak bond connecting flexible polymer chains. *Biophysical Journal* **76**, 2439–2447.

Florin, E. L., Moy, V. T. & Gaub, H. E. (1994). Adhesion forces between individual ligand–receptor pairs. *Science* **264**, 415–417.

Hansma, H. G. & Pietrasanta, L. (1998). Atomic force microscopy and other scanning probe microscopies. *Current Opinion in Chemical Biology* **2**, 579–584.

Hinterdorfer, P., Baumgartner, W., Gruber, H. J., Schilcher, K. & Schindler, H. (1996). Detection and localization of individual antibody–antigen recognition events by atomic force microscopy. *Proceedings of the National Academy of Sciences of the USA* **93**, 3477–3481.

Hynes, R. O. (1999). The dynamic dialogue between cells and matrices: Implications of fibronectin's elasticity. *Proceedings of the National Academy of Sciences of the USA* **96**, 2588–2590.

Improta, S., Krueger, J. K., Gautel, M., Atkinson, R. A., Lefevre, J. F., Moulton, S., Trewhella, J. & Pastore, A. (1998). The assembly of immunoglobulin-like modules in titin: implications for muscle elasticity. *Journal of Molecular Biology* **284**, 761–777.

Improta, S., Politou, A. S. & Pastore, A. (1996). Immunoglobulin-like modules from titin I-band: extensible components of muscle elasticity. *Structure* **4**, 323–337.

Lee, G. U., Chrisey, L. A. & Colton, R. J. (1994). Direct measurement of the forces between complementary strands of DNA. *Science* **266**, 771–773.

Li, H., Rief, M., Oesterhelt, F. & Gaub, H. E. (1998). Single-molecular force spectroscopy on xanthan by AFM. *Advanced Materials* **3**, 316–319.

Lu, H., Isralewitz, B., Krammer, A., Vogel, V. & Schulten, K. (1998). Unfolding of titin immunoglobulin domains by steered molecular dynamics simulation. *Biophysical Journal* **75**, 662–671.

Marszalek, P. E., Oberhauser, A. F., Pang, Y. P. & Fernandez, J. M. (1998). Polysaccharide elasticity governed by chair-boat transitions of the glucopyranose ring. *Nature* **396**, 661–664.

Moy, V. T., Florin, E. L. & Gaub, H. E. (1994). Intermolecular forces and energies between ligands and receptors. *Science* **266**, 257–259.

Murray, A. J., Head, J. G., Barker, J. J. & Brady, R. L. (1998). Engineering an intertwined form of CD2 for stability and assembly. *Nature Structural Biology* **5**, 778–782.

Oberhauser, A. F., Marszalek, P. E., Carrion-Vasquez, M. & Fernandez, J. M. (1999). Single protein misfolding events captured by AFM. *Nature Structural Biology* (in the Press).

Oberhauser, A. F., Marszalek, P. E., Erickson, H. P. & Fernandez, J. M. (1998). The molecular elasticity of the extracellular matrix protein tenascin. *Nature* **393**, 181–185.

Ohashi, T., Kiehart, D. P. & Erickson, H. P. (1999). Dynamics and elasticity of the fibronectin matrix in living cell culture visualized by fibronectin-green fluorescent protein *Proceedings of the National Academy of Sciences of the USA* **96**, 2153–2158.

Palecek, S. P., Loftus, J. C., Ginsberg, M. H., Lauffenburger, D. A. & Horwitz, A. F. (1997). Integrin-ligand binding properties govern cell migration speed through cell-substratum adhesiveness. *Nature* **385**, 537–540.

Politou, A. S., Thomas, D. J. & Pastore, A. (1995). The folding and stability of titin immunoglobulin-like modules, with implications for the mechanism of elasticity. *Biophysical Journal* **69**, 2601–2610.

Rief, M., Clausen-Schaumann, H. & Gaub, H. E. (1999). Sequence-dependent mechanics of single DNA molecules. *Nature Structural Biology* **6**, 346–349.

Rief, M., Gautel, M., Oesterhelt, F., Fernandez, J. M. & Gaub, H. E. (1997*a*). Reversible unfolding of individual titin immunoglobulin domains by AFM. *Science* **276**, 1109–1112.

Rief, M., Gautel, M., Schemmel, A. & Gaub, H. E. (1998). The mechanical stability of immunoglobulin and fibronectin III domains in the muscle protein titin measured by atomic force microscopy. *Biophysical Journal* **75**, 3008–3014.

Rief, M., Oesterhelt, F., Heymann, B. & Gaub, H. E. (1997*b*). Single molecule force spectroscopy on polysaccharides by atomic force microscopy. *Science* **275**, 1295–1297.

Shao, Z. & Yang, J. (1995). Progress in high resolution atomic force microscopy in biology. *Quarterly Reviews of Biophysics* **28**, 195–251.

Smith, B. L., Schaffer, T. E., Viani, M., Thompson, J. B., Frederick, N., Kindt, J., Belcher, A., Stucky, G. D., Morse, D. E. & Hansma, P. K. (1999). Molecular mechanistic origin of the toughness of natural adhesives, fibers, and composites. *Nature* **399**, 761–763.

Weber, T., Zemelman, B. V., McNew, J. A., Westermann, B., Gmachl, M., Parlati, F., Sollner, T. H. & Rothman, J. E. (1998). SNAREpins: minimal machinery for membrane fusion. *Cell* **92**, 759–772.

Acknowledgements

This work was supported by NIH grant R01 NS 35866 (to J.M.F.).

Corresponding author

J. M. Fernandez: Department of Physiology and Biophysics, Mayo Foundation, 1-117 Medical Sciences Building, Rochester, MN 55905, USA.

Email: fernandez.julio@mayo.edu